Lab on a Chip

RSC Publishing

PAPER

View Article Online
View Journal | View Issue

Cite this: *Lab Chip*, 2013, **13**, 2075

Genotyping of single nucleotide polymorphisms by melting curve analysis using thin film semi-transparent heaters integrated in a lab-on-foil system

Anna Ohlander,*[a] Caterina Zilio,[b] Tobias Hammerle,[a] Sergey Zelenin,[d] Gerhard Klink,[a] Marcella Chiari,[b] Karlheinz Bock[ac] and Aman Russom[d]

Received 6th February 2013,
Accepted 18th March 2013

DOI: 10.1039/c3lc50171j

www.rsc.org/loc

The recent technological advances in micro/nanotechnology present new opportunities to combine microfluidics with microarray technology for the development of small, sensitive, single-use, point-of-care molecular diagnostic devices. As such, the integration of microarray and plastic microfluidic systems is an attractive low-cost alternative to glass based microarray systems. This paper presents the integration of a DNA microarray and an all-polymer microfluidic foil system with integrated thin film heaters, which demonstrate DNA analysis based on melting curve analysis (MCA). A novel micro-heater concept using semi-transparent copper heaters manufactured by roll-to-roll and lift-off on polyethylene naphthalate (PEN) foil has been developed. Using a mesh structure, heater surfaces have been realized in only one single metallization step, providing more efficient and homogenous heating characteristics than conventional meander heaters. A robust DNA microarray spotting protocol was adapted on Parylene C coated heater-foils, using co-polymer poly(DMA-NAS-MAPS) to enable covalent immobilization of DNA. The heaters were integrated in a microfluidic channel using lamination foils and MCA of the spotted DNA duplexes showed single based discrimination of mismatched over matched target DNA-probes. Finally, as a proof of principle, we perform MCA on PCR products to detect the Leu7Pro polymorphism of the neutropeptide Y related to increased risk of Type II diabetes, BMI and depression.

Introduction

The application of genetic markers as unique fingerprints for specific traits or certain medical conditions has revolutionized medicine and evolutionary research. Single nucleotide polymorphism (SNP) is the most common genetic variation between individuals and is one of the promising candidates to be used as such. Until now, millions of human SNPs have been discovered and susceptibility loci associated with a number of conditions have been characterized, including alcohol dependency, bipolar disorder, height and eye color.[1–4] Using SNPs as markers in disease diagnostics can improve healthcare by increasing detection accuracy and efficiency and hence promote faster diagnosis and the correct treatment of patients. As an example, recently, five specific SNPs were identified as genetic markers for lethal prostate cancer paving the way towards early cancer diagnosis through a simple blood test.[5] Through the set of five SNPs, it was possible to distinguish between aggressive prostate cancers and more indolent ones. Hence, through this it would be possible to adjust medication according to the type of cancer and spare patients with a milder form of the illness having to go through unnecessarily painful treatments. However, SNPs do not only reside in the human genome, but are also as frequent in many important human and agricultural pathogens making them applicable in the battle against pandemics. R. Daniels *et al.* have identified 24 SNPs to serve as a molecular bar code for the detection and tracking of the malaria parasite *P. Falciparum*.[6] Furthermore, scientists have used SNPs to study the development of antiviral resistance during the 2009 pandemic H1N1 influenza virus.[7]

In general, there are five fundamental strategies for SNP screening and detection; hybridization-based, through allele-specific PCR, by primer extension, ligation or endonuclease cleavage.[8] Among these techniques, melting curve analysis (MCA) has been proven to be a robust technique to apply in clinical applications.[9] It relies on real time monitoring of denaturing DNA duplexes in solution or immobilized on to a solid support, exposed to a thermal gradient. Whilst remaining a simple hybridization assay without the need of any additional chemicals or specific enzymes, it is not dependant

[a]*Fraunhofer EMFT, Hansastrasse 27d, 80686 Munich, Germany. E-mail: anna.ohlander@emft.fraunhofer.de; Tel: +498954759233*
[b]*Institute of Biocatalysis and Molecular Recognition, CNR, Via Mario Bianco 9, 20131 Milan, Italy*
[c]*University of Berlin, Center for Technologies of Microperipherics, Chair of PolytronicMicrosystems, Gustav-Meyer Allee 25, D-13355 Berlin, Germany*
[d]*Division of Proteomics and Nanobiotechnology, Science for Life Laboratory, KTH Royal Institute of Technology, Sweden*

on the use of redundant probes to be able to distinguish a mutation on a single base level as in the case of SNP microarray technology.

Miniaturization provides a way to increase throughput at a lower cost. DNA microarrays offer massive parallel solid-phase assays, while microfluidics offers homogeneous assays which can be miniaturized. As an example, the Affymetrix's Genome-Wide Human SNP Array 6.0 includes probes for 906 600 SNPs and 946 000 non-polymorphic copy number probes. However, the platform is prohibitively expensive and limited to laboratories with the need for large scale, massive parallel analysis. Point-of-care molecular diagnostics on the other hand, has fewer requirements on parallelization and more on sample integration. Merging microfluidics and microarrays, two powerful technologies, is therefore attractive for diagnostic applications as the integration of active fluidics offers the ability to manipulate exceptionally small volumes of liquid in an integrated fashion, whereas microarray technology promotes the multiplexing of experiments. The result is low reagent consumption, short analysis times, improved sensitivity and high-throughput of the analysis. In addition, these systems can be mass-fabricated at a low cost, especially when polymer-based materials are used in their construction. High volumes of disposable devices can be produced by relatively inexpensive micro-injection molding, as opposed to the expensive silicon etching needed to make lab-on-chips. In an effort to replace the well-established glass substrate material for microarrays, several polymers have been investigated for DNA immobilization, including cyclic olefin copolymer (COC), poly(methyl methacrylate) (PMMA), polycarbonate (PC), polystyrene and poly(ethylene terephthalate) (PET).[10–13]

The use of polymer foils has gained increased interest in the past few years as it opens up for roll-to-roll manufacturing as an alternative high throughput production technology. Beyond cost efficient manufacturing, foils possess benefits in terms of efficient heat transfer due to the thin walls of the system. The mechanical flexibility can be used for effective liquid transportation in the system by external actuation and can promote easier assembly. Many of the popular lab-on-chip polymer materials are also available as thin foils. Consequently, lab-on-foil fabrication technologies are to a large extent analogous to rigid plastic cartridge manufacturing, where various technologies, such as thermoplastic processing, dry-resist technologies, laser machining and lamination can be applied to form fluidics and microstructures. Recently, a roll-to-roll hot embossed electrophoresis chip for antibiotic resistance detection in bacteria was developed.[14] Furthermore, the company Micronic Inc. has taken their lamination-based Lab-Card concept for applications, such as ABO blood typing and cancer diagnostics, to the market.[15–17] An overview of lab-on-foil technologies, can be found in a recent review by M. Focke *et al.*[18]

Although miniaturizing a biological assay is not straightforward, a major advantage of miniaturizing MCA is that the very low thermal mass of the surface enables the sample to be very rapidly heated. Precise and rapid temperature control is more easily obtained at the micro-scale than at macro-scale dimensions. We have previously shown MCA on monolayers of beads using a glass-based system with integrated heaters and sensors manufactured by conventional MEMS fabrication technologies.[19,20] G. Vecchio *et al.* developed a chip consisting of two modules in PDMS coupled to external reusable thermal cycling units for PCR and subsequent MCA detection of human papilloma virus.[21] The approach of separating disposable chip and reusable heating units is often seen in plastic PCR chips.[22–26] One reason for this is that conventional MEMS manufacturing technologies are less compatible with common lab-on-chip substrates making integration of electronic features sometimes difficult in polymer systems. Using external heating, on the one hand reduces the number of fabrication steps of the chip, but on the other hand, makes thermal contact between the chip and heating block, and heat transfer through plastic materials with low thermal conductance, a critical issue to obtain fast heating rates and thermal accuracy.

Optical transparency of the substrate is often a desired feature in lab-on-chips, as it facilitates online monitoring and observation of an assay. Transparent heaters for PCR and cell cultivation assays have been produced by structuring Indium-tin-oxide (ITO) on glass.[27–30] Indium, being a rare earth element, is however relatively expensive and hence unsuitable for low-cost diagnostic purposes.

In this paper, we introduce a system merging the need for integrated heating, optical transparency and low-cost manufacturing technologies using foil substrates and thin film metallization. This is done using a novel heater concept consisting of a copper mesh integrated in a microfluidic foil system. Furthermore, we show the functionalization of parylene-coated foil heaters using a co-polymer of *N*,*N*-dimethylacrylamide (DMA), *N*-acryloyloxy-succinimide (NAS) and [3-(methacryloyl-oxy)propyl-trimethoxy-silane] (MAPS), for straight forward covalent immobilization of DNA.[31] We first demonstrate MCA of the microarray spotted DNA duplexes, showing clear discrimination of matching, mismatching and heterozygous oligonucleotides. Finally, as a proof of principle, we perform MCA on PCR products to detect the Leu7Pro polymorphism of the neuropeptide Y related to an increased risk of Type II diabetes, BMI and depression.[32–34]

Materials and methods

Heater fabrication and characterization

Mesh and meander heaters were structured on a 125 μm thick planarized PEN foil (Teonex, DuPont Teijin Film) in a roll-to-roll processing mode in the following way. A 15 nm Ti adhesion layer and 100 nm Cu was deposited onto the PEN foil by sputtering (FHR Rollcoater RC200+) followed by roll-to-roll photolithography and wet etching (Optoline 200 Ciposa SA, Höllmüller, Schmidt). Mesh and meander heaters were also structured sheet wise, on the same type of PEN foil in a double resist lift-off process using LOR 7B (Micro Chem) and AZ1514H (Clariant). The Ti and Cu were in this case evaporated using a BAK 760 evaporator (Balzer). All heaters

were designed with a four-point connection for power supply and sensing and an overall heater surface of 1.5 × 3 mm^2, but with varying line/space ratios. For encapsulation, a 2 μm thick layer of Parylene C was deposited by a CVD process on the heaters (PDS 2010 Labcoter 2, SCS Specialty Coating System). The contacts were covered with tape for accessibility.

The contour of the fluidic channels was cut in a 50 μm thick pressure sensitive double-sided adhesive tape (ARSeal 90880, Adhesive Research Inc.) by a UV-laser with a wavelength of 355 nm (LS Lasersystem GmbH).

The thermal coefficient of resistance (TCR) of the heaters was measured by cycling the heaters between 0 and 100 °C, while monitoring the resistance.

For heating, the heaters were connected to a Kiethley 2400 SMU (Source Measure Unit). The heaters were controlled by applying an in-house developed software using Agilent VEE, based on a standard PID controller.

The surface temperature of the heaters was achieved by attaching a Pt1000 sensor onto the heater surface, while increasing the temperature by the desired rate for the MCA.

To evaluate the thermal distribution in the different heater designs, a 15 μm thick layer of encapsulated thermo-chromic liquid crystals (TLC), (LCR Hallcrest) was spin-coated on the heaters. Heaters were heated and kept at 62 °C, while observing the color changes under a microscope (Zeizz, Axioplan 2 Imaging). The experiment was repeated for 2 samples of each design.

DNA probe and target preparation

The oligonucleotides and probes (biomers. net, Ulm, Germany) had the following sequences: Allele-specific probe: 5′-Cy3ACACAAAC(**G**)CTGTTGGA-3′; 55 bases long matched target-DNA: 5′-Aminolink-ATGAGAGAAGAGAGACTATTTTCCA-ACAG(**C**)GTTTGTGTTTCTTGGATGTCATTCT-3′; and mismatched target-DNA: 5′-Aminolink-ATGAGAGAAGAGAGACTA-TTTTCCAACAG(**G**)GTTTGTGTTTCTTGGATGTCTCT-3′. The SNP position is highlighted in bold.

The sequences of PCR primers were derived from a previously published NPY genotyping assay.[32] In the current study however, we have adapted a protocol that enables direct analysis of the PCR product *via* hybridization to pre-spotted allele-specific probes. The matched and mismatched oligonucleotide probes immobilized to the heater surface had the following sequences: 5′-Aminolink-TTTTTTTTTTTTTTTTCAA-GTGAC(**T**/**C**)GGGGCTGT. The 15-mer-polyT between the surface and allele-specific sequence acts as a spacer arm. For the PCR product preparation, blood was drawn from healthy donors and collected in venous blood collection tube containing EDTA (BD vacutainer, BD bioscience) at the Blood Centre Skanstull (Stockholm, Sweden) and genomic DNA was purified using DNeasy Blood & Tissue Kit (QIAGEN) according to the manufacturer's protocol. The purified DNA samples were then stored at −20 °C, ready to be used as a template for the PCR. A nested PCR was used to prepare Cy3-labeled, single stranded PCR product with the sequence: 5′-Cy3GCGAGAGTCA-GTCCAGACAGCCCC(**G**)GTCACTTGTTACCTAGCATCTGC-3′. The SNP position is highlighted in bold. For the nested PCR, genomic DNA (14 ng) was amplified in 100 μl of PCR mixture containing 1 × Pfx amplification buffer (Invitrogen), 1 mM $MgSO_4$, 0.3 mM of each dNTP, 2.5 units of Pfx DNA polymerase (Invitrogen) and 0.2 μM of forward and reverse PCR primers. PCR cycles started with enzyme activation at 94 °C for 4 min followed by 35 cycles (denaturation at 94 °C for 15 s, annealing at 55 °C for 30 s and elongation at 68 °C for 30 s). The PCR fragments were purified using 2% agarose gel and eluted by GeneJET™ Gel DNA Extraction Kit (Fermentas). The PCR product was then used as a template to produce the final Cy3-labeled PCR by asymmetric PCR amplification. Except for the primer concentrations, 28 nM reverse primer and 0.2 μM of forward primer, all conditions were the same as for the first round of PCR described above. The forward primer was labeled with Cy3 at the 5′-end. The final PCR products were separated on 2% agarose gel and purified using GeneJET™ Gel DNA Extraction Kit (Fermentas).

Surface functionalization and arraying

For covalent attachment of oligonucleotide probes onto the heater surface, the parylene surface was functionalized with poly(DMA-NAS-MAPS), which bears active esters capable of binding to amino-modified oligonucleotides. The parylene surfaces were oxidized by plasma treatment at 1.2 bar and 29.6 W for 10 min in a plasma cleaner, (Harrick Plasma, Ithaca, NY, USA). Immediately after oxygen plasma treatment, the ox-heaters were immersed in a 1% w/v solution of poly-(DMA-NAS-MAPS) in ammonium sulfate at 20% of the saturation level. After rinsing in DI water and drying in nitrogen, the heaters were cured in vacuum at 80 °C for 15 min. Amino-modified match and mismatch oligonucleotides were dissolved in sodium phosphate buffer (150 mM, pH 8.5) to a final concentration of 10 μM. A solution of 50/50 matched and mismatched target DNA was prepared to simulate a heterozygous sample. Spotting was performed using a noncontact microarray spotter SCIENION sciFLEXARRAYER S5 assembled with an 80 μm nozzle. The heaters were blocked with 50 mM ethanolamine in 0.1 M TRIS/HCl buffer (pH 9) at room temperature for 1 h. The oligo-spotted heaters were incubated with the Cy3-labeled complementary target at a concentration of 1 μM for 2 h at room temperature. For the PCR experiments, matched and mismatched probes were spotted in the same way as described above in a concentration of 10 μM. For hybridization, a double-sided adhesive tape 50 μm thick with the contour of a channel (1.8 mm width) was placed on the heater, followed by lamination of a 125 μm thick PEN foil to close the system. The channel was filled with a 1 : 1 solution of PerfectHyb (Sigma Aldrich) and the Cy3-labeled single stranded PCR product. The concentration of the PCR product was 7 pM. The system was left to hybridize over night at 38 °C. The channel was rinsed with 0.1 × SSC with 0.1% SDS before performing the MCA.

Melting curve analysis

The heaters were assembled under a microscope (Zeizz, Axioplan 2 Imaging) and connected to the Kiethley 2400 SMU/Agilent VEE set up as described earlier. On the open heaters spotted with oligonucleotide samples, a drop of 5 × SCC buffer was applied on the heater surface and covered with a glass slide. The channels with integrated heaters spotted with NPY probes were filled with the same buffer. Heaters were

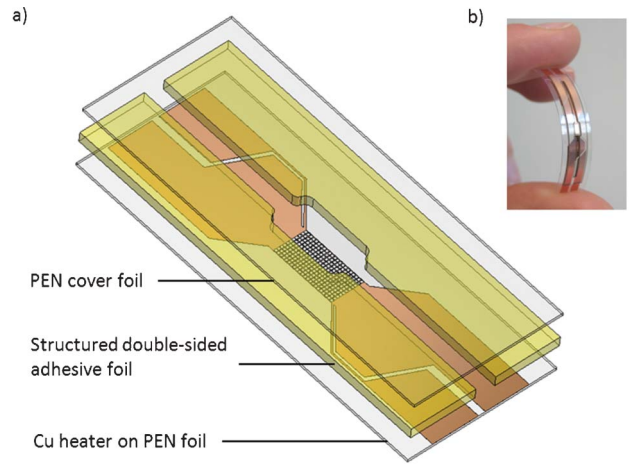

Fig. 1 (a) A schematic representation of a lab-on-foil system for SNP detection by melting curve analysis. A microarray of SNP specific oligonucleotides are spotted in the center of the mesh heater. (b) Integrated copper thin film heater in a microfluidic system entirely made of plastic foils.

ramped from room temperature to 100 °C at a speed of 8 °C min^{-1}, while following the intensity decay by manually taking microscope images every ten seconds. Pictures were evaluated using ImageJ to extract intensity profiles and the data was analyzed using Origin 8.

Results and discussion

In this project, we are investigating an all-plastic foil microfluidic system with an integrated thin film metal heater for MCA. A schematic picture of the system is shown in Fig. 1.

The system consists of a copper mesh heater structured on a transparent 125 μm thick PEN foil. The heater is electrically insulated by a 2 μm thick layer of Parylene C. A microfluidic contour is structured using a laser in a 50 μm thick double-sided adhesive tape and laminated onto the heater, and a second PEN foil seals the device. The mesh heater surface is 1.5 × 3 mm^2 and is designed with a four-point connection for power supply and temperature sensing. The use of a mesh structure has several advantages, including a higher manufacturing robustness as the device's functionality is not relying on one single metal conductor, low power consumption and assumed improved thermal characteristics compared to a conventional meander heater design. For the MCA, a microarray of allele-specific probes are covalently immobilized on the Parylene C coated mesh heater using poly-(DMA-NAS-MAPS) followed by hybridization of a fluorescently labelled target. By increasing the temperature in the mesh at a controlled rate, the heat will dissociate the immobilized DNA. The result is a decay in fluorescence intensity as a consequence of the labelled targets dissociating away from the surface. A single base point mutation in a DNA duplex causes decay at a lower temperature compared to perfectly matching DNA strands.

Thermal characterization

For the heaters to be applicable for MCA, thermal homogeneity on the surface where the DNA oligonucleotides are immobilized is crucial as the temperature is being used to discriminate between SNPs. Mesh and meander heaters with varying line/space ratios and a total heater footprint of 1.5 × 3 mm^2 were processed either by roll-to-roll wet etching or sheet-wise by lift-off. To compare the thermal distribution between a conventional meander structure and a mesh, and the effect of reducing the mesh size, a 15 μm thick TLC layer was spin coated on the heaters and dried. The heaters were assembled under a microscope and heated to a temperature in the active interval of the TLCs (60–65 °C). In Fig. 2, the color changes in the TLC layer of the three different heater designs at 62 °C, after image processing, can be seen. The current is applied from A to B on the large contact pads, whereas the thin ones are used for sensing and control. In all three cases, a hot spot in the TLC layer is produced with a temperature difference of about 2 °C from center to edge on the heater. However, the hot spot in the meander heater (Fig. 2b) creates a more circular thermal profile than the mesh heaters in Fig. 2d and f, which tend to have a more square shaped heat profile. This indicates a more efficient heat spreading over the total heater surface using a mesh design. The hot wires are clearly visible in both the meander and the large mesh structure (b and d).

In the meander heater however, the hot wires are vertical to the length of the rectangle making heat spread less efficiently along the length of the rectangular heater surface. This is because the generated heat in the copper wires has several Cu/PEN (high thermal conductivity/low thermal conductivity) boundaries to overcome from A to B. In the 15/150 μm line/space mesh heater, the hot conductors are also visible, but are in line with the contact pads, hence the heat encounters less resistance between A and B. It is assumed that the perpendicular conductors assist in spreading the heat in the vertical direction. However, more experiments are needed to confirm this. A design using only parallel conductors could be used for this purpose. By reducing the line/space ratio by a factor of three (Fig. 2e and f), the metal conductors are less reproduced in the TLC layer indicating higher thermal homogeneity at the micro-scale than in the large mesh in Fig. 2c and d. The increased thermal homogeneity is likely the result of two factors. Reducing the copper wire from 15 to 5 μm in width leads to increased resistance in the wire, meaning increased joule heating and higher heat dissipation from it. By reducing the space between the copper wires, the distance for the heat to spread in the plastic substrate with low thermal conductance is shorter, hence thermal homogeneity can be achieved more effectively. The thermal characteristics discussed above were observed for each set of two heaters for each heater design. The mesh design clearly exhibits advantageous characteristics in terms of heat spreading over the surface both at the macro- and micro-scale. Using the mesh heater concept for lab-on-chip applications could further be optimized by exploring other heating materials and plastic substrates with different thermal characteristics than the copper and PEN used. A consideration in material selection could also additionally lower the cost. Reducing the line/space

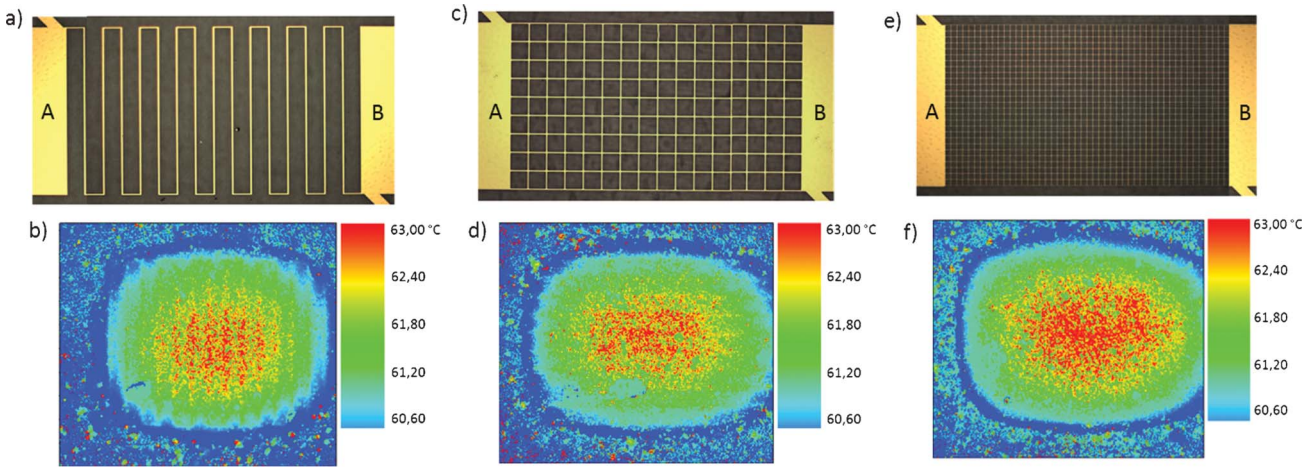

Fig. 2 (a) Roll-to-roll manufactured Cu meander heater with 15 μm lines and 150 μm spaces on 125 μm PEN foil. The transparent foil is put on a dark background for clarity. (b) The corresponding thermal profile at the surface in (a) at 62 °C using a 15 μm thick TLC layer. The current bearing conductors are clearly visible. (c) Roll-to-roll manufactured mesh heater with 15 μm lines and 150 μm spaces on PEN foil. (d) The TLC response of the mesh heater in (c) at 62 °C. The hot spot in the heater has a more rectangular shape than in (b) indicating a more efficient heat spreading related to the 1.5 × 3.0 mm^2 heater surface. (e) Lift-off processed mesh heater with 5 μm lines and 50 μm spaces on PEN foil. (f) The color changes in the TLC layer coated on the heater in (e). As in (d) the hot spot has a rectangular shape. The mesh pattern is however less reproduced in the thermal image compared to (d) indicating a more homogenous heat spreading on the micro-scale by reducing the mesh size.

ratios would further improve the thermal homogeneity, but is dependant on the limitations in the manufacturing technology used.

DNA arraying

To integrate DNA microarrays within a microfluidic device, there is a need for the development of a robust surface modification approach that is compatible with the microfabrication method. As the MCA is a solid phase assay that involves dynamic heating, while measuring the transition of DNA duplexes, reliable immobilization of the probe to the solid support is even more crucial for an accurate measurement. As mentioned in the introduction, several groups have investigated polymers as potential supports for microarray production, including COC, PMMA, PC and PET to enable biomolecule binding. Typically, the formation of –COOH groups on the plastic surface is achieved by UV irradiation. For our application, it is required that the microarray in addition is integrated on a thin film micro-heater. The micro-heater in turn needs to be electrically insulated towards the buffer solution for its functionality. Parylene C is a classical MEMS material, which due to its inertness, chemical resistance, barrier and conformal coating properties finds applications within a wide variety of industries. In the medical industry, it is used as a coating material for catheters, stents and implants and in the MEMS area, it is a common dielectric and passivation material, which lately also has gained interest as a material for bioMEMS. Its inertness, which as just mentioned is favorable in many aspects, makes it however less prone to surface modification, which can be a draw back for many biosensor applications. Previously, we have reported on the use of copolymerized substrates using co-polymer poly(DMA-NAS-MAPS) to activate various surfaces, such as PDMS and nitrocellulose.[35,36] To enable covalent immobilization of the DNA probe onto the Parylene C coated thin film heaters, co-polymer poly(DMA-NAS-MAPS) was introduced. This copolymer, obtained by radical polymerization of dimethylacrylamide (DMA), *N*-acryloyl-oxy-succinimide (NAS) and 3-(trimethoxysilil)propyl-methacrylate (MAPS), forms a thin film on the surface of Parylene C by physi-/chemisorption.[31] The film bears active esters that allow covalent binding of amino-modified oligonucleotides. After functionalization and probe spotting, the surfaces were blocked using ethanolamine followed by hybridization of the target strand. In Fig. 3, an array of match, mismatch and heterozygous spots on a mesh heater can be seen. The hybridized DNA spots 150 μm in diameter are clearly visible due to the Cy3-labeling. To the author's knowledge, few examples can be found in the literature where covalent biomolecular immobilization on Parylene C surfaces has been achieved. All found examples are based on the amino-modified Parylenes DixA and DixAM provided by the company Kisco.[37,38] However, through co-

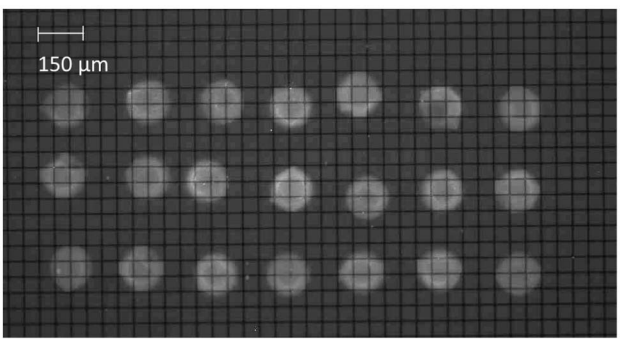

Fig. 3 Match, heterozygous and mismatch oligonucleotides immobilized onto a Parylene C coated mesh heater with 5 μm lines and 50 μm space.

polymer poly(DMA-NAS-MAPS), we have modified Parylene C, which as raw material, is cheaper than DixA and DixAM, in a robust way in only about 30 min. Although more experiments are required to fully evaluate the immobilization protocol using optimized spotting techniques with high spot homogeneities for other microarray analyses, the spotted arrays were able to withstand several washing steps and temperature increase up to 100 °C without detaching from the surface, hence the protocol is ideally suited for a MCA analysis.

Melting curve analysis

Based on the thermal mapping using TLC, it was concluded that the mesh heater with 5 μm lines and 50 μm space was the best suited for further experiments due to its supreme thermal characteristics relative the other designs. To investigate its dynamic heating properties and prove its feasibility for MCA, a model DNA system using synthesized oligonucleotides was used.

An area of 750 × 1000 μm^2 in the center of the heater was defined as the active area having the thermal homogeneity adequate for the experiments. Synthesized oligonucleotide targets (matched, mismatched- and a 50/50% mixture of the two) were spotted on mesh heaters as in Fig. 3. After hybridization with the complementary probe and subsequent washing, the temperature was increased in the heater and the fluorescence intensity was measured by manually taking pictures using a microscope CCD camera every 10 s. Using the PID-based controller software, it was possible to increase the temperature of the heaters at a stable and defined rate. As copper easily oxidizes, this indicates that the insulation using Parylene C is working satisfyingly. Without proper insulation, the copper wire oxidizes upon heating and interaction with the environment resulting in a continuous change in resistance in the circuit. This gives an incorrect feedback value for the PID controller resulting in instable behavior of the heater. Fig. 4 shows normalized fluorescence intensity plotted against temperature for 4 matched, 3 mismatched and 3 heterozygous samples in the active (750 × 1000 μm^2) spot area. The green, blue and red colored curves are from individual microarray spots, while the black curves shows the average signal from each sample type. As can be seen in the graph, there is a clear distinction between matched, mismatched and heterozygous samples. The single base mismatch causes duplex instability and dissociation at a lower temperature than the matching duplex. In the heterozygous case, both a matching and a mismatching allele is present in the gene at the single polymorphism position, hence, a signal from both match and mismatch is produced as a result of super positioning of the individual match and mismatch intensity signals. The results show, that the heater concept using a thin film copper mesh on a PEN foil can be used for MCA to detect SNPs. Even though the spots are distributed over a 750 × 1000 μm^2 area, a clear distinction between the averaged curves can be made, proving that the thermal homogeneity is adequate for single base discrimination for SNP detection on the surface where the targets are immobilized. The reproducible melting curves for each of the sample can be further improved by optimizing the mesh design. Further, the result consolidates the use of co-polymer poly(DMA-NAS-MAPS) as a robust immobilization method of the DNA probes on the parylene-coated heater surface.

For point-of-care molecular diagnostics, there is a need to perform MCA on clinical relevant samples using PCR products from genomic DNA. As a proof of principle, the SNP of the human neuropeptide Y (NPY) gene was tested. The matched and mismatched probes were spotted symmetrically in two rows in the active area of the mesh (5 μm lines with 50 μm spaces) micro-heater. Before hybridization with the complementary strand, a channel cut in double-sided adhesive tape was laminated onto the heater foil and the system was closed with a second PEN foil. The Cy3-labeled target was injected by syringe and left to hybridize. Fig. 5 shows the melting curve analysis of 4 match and 4 mismatch spots on a mesh heater

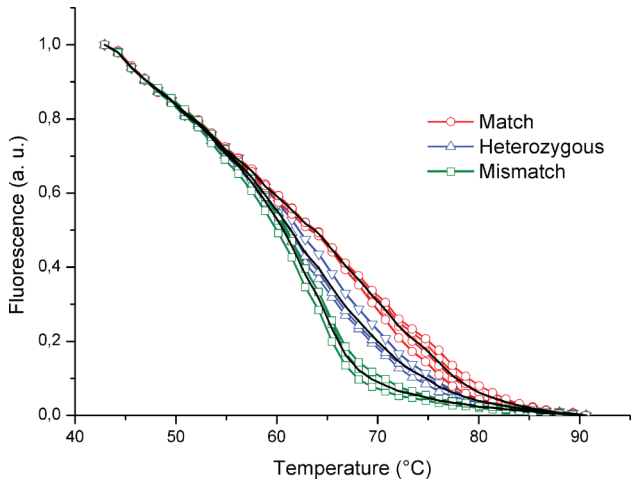

Fig. 4 SNP genotyping based on MCA. The normalized fluorescence intensity of 4 matched, 3 mismatched and 3 heterozygous spots plotted against temperature. The black curves show the average of respective sample types. All three SNP variations are clearly distinguishable.

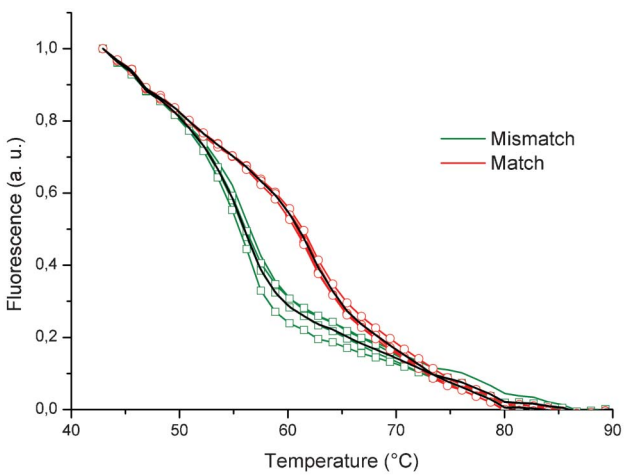

Fig. 5 Detection of the PreproNPY gene polymorphism. Normalized intensity of four matched and four mismatched samples. The black line shows the average intensity for the respective alleles.

surface and the average of the curves (black). Again, a clear discrimination can be made between the matching and the mismatching alleles. The substitution of a thymine to a cytocine base in the mismatching sample causes the probe-target duplex to dissociate at a lower temperature than the matching one. Although the centre-to-centre distance between the first and the fourth spot in the two rows of spots is as large as 900 μm, the match and the mismatch curves are highly reproducible, which again proves thermal homogeneity in the defined heater surface area used for analysis.

By integrating the heaters in a microfluidic channel, we open up the possibility of integration of the detection principle in a complete sample-to-answer microfluidic chip. Using a simple copper mesh we have created a heater, which provides the thermal homogeneity required for the MCA in only one metallization step using a fairly cheap metal. The mesh heater provides a more robust design from a manufacturing point of view, while also being semi-transparent. This opens up possibilities to develop cheaper alternative detection principles to fluorescence, such as monitoring of micro- and nanoparticles coupled through biotin–streptavidine chemistry. In this way, a simple transmission/absorption measurement could be made to monitor the melting of the duplexes without the need for expensive and bulky laboratory microscopes and fluorescent markers, which further promotes a reduction of the analysis cost. Finally, an additional advantage of using a mesh structure rather than a meander is the heavy reduction in voltage supply needed, which is important for portable applications. Obtaining the same thermal and optical characteristics as the 5/50 mesh, but using a meander structure, rendered resistance in the kOhms range. It would require a very high voltage to be able to perform the MCA using such a design. However, a high voltage power supply may be a limiting factor in field deployable settings. It is therefore favorable to use a mesh design for point-of-care applications. To power up the 5/50 mesh heaters to 100 °C during the MCA experiments, less than 2 V was required.

Conclusion and outlook

We have, for the first time, demonstrated the detection of SNPs on thin film heaters fully integrated in an all-plastic foil microfluidic system. Using a novel mesh heater concept, a semi-transparent heater on foil has been created in only one metallization step, which provides the thermal homogeneity needed for the analysis. With a non-optimized heating rate of 8 °C min^{-1}, successful MCA on oligonucleotides, as well as PCR products, were obtained in a total analysis time of 5 min. These results clearly demonstrate the merging of microarray technologies and low-cost roll-to-roll processed foil microfluidics as a feasible concept for point-of-care molecular diagnostics.

References

1 L. Bierut, A. Agrawal and K. Bucholz, *Proc. Natl. Acad. Sci. U. S. A.*, 2010, **11**, 5082–5087.
2 P. Sklar, J. W. Smoller and J. Fan, *Mol. Psychiatry*, 2008, **13**(6), 558–69.
3 S. Sanna, A. Jackson and R. Nagaraja, *Nat. Genet.*, 2008, **40**(2), 198–203.
4 M. Kayser, F. Lui and C. Janssens, *Am. J. Hum. Genet.*, 2008, **82**, 411–423.
5 D. Lin, L. FitzGerald and R. Fu, *Cancer Epidemiol., Biomarkers Prev.*, 2011, **20**(9), 1928–1936.
6 R. Daniels, S. Volkman and D. Milner, *Malar. J.*, 2008, **7**, 223.
7 S. Duan, D. Boltz and J. Li, *Antimicrob. Agents Chemother.*, 2011, **55**(10), 4718–4727.
8 AC. Syvänän, *Nat. Rev. Genet.*, 2001, **2**, 930–942.
9 L. Strömqvist Meuzeelar, K. Hopkins and E. Liebana, *J. Mol. Diagn.*, 2007, **9**(1), 30–41.
10 K. Kinoshita, K. Fujimoto and T. Yakabe, *Nucleic Acids Res.*, 2006, **35**, e3.
11 D. Sabourin, J. Petersen and D. Snakenborg, *Biomed. Microdevices*, 2010, **12**, 673–681.
12 Y. Li, Z. Wang and L. M. L. Ou, *Anal. Chem.*, 2007, **79**, 426–433.
13 N. Kimura, *Biochem. Biophys. Res. Commun.*, 2006, **347**, 477–484.
14 R. Liedert, L. K. Amundsen and A. Hokkanen, *Lab Chip*, 2012, **12**, 333–339.
15 B. Weigl, G. Domingo and P. LaBarre, *Lab Chip*, 2008, **8**, 1999–2014.
16 M. Kokoris, M. Nabavi and C. Lancaster, *Methods*, 2005, **37**, 114–119.
17 C. Lancaster, M. Kokoris and M. Nabavi, *Methods*, 2005, **37**, 120–127.
18 M. Focke, D. Kosse and C. Müller, *Lab Chip*, 2010, **10**, 1365–1386.
19 A. Russom, S. Haasl and A. Ohlander, *Electrophoresis*, 2004, **25**, 3712–3719.
20 A. Russom, S. Haasl and A. J. Brookes, *Anal. Chem.*, 2006, **78**, 2220–2225.
21 G. Vecchio, S. Sabella and L. Tagliaferro, *Anal. Biochem.*, 2010, **397**, 53–59.
22 K. H. Chung, S. H. Park and Y. H. Choi, *Lab Chip*, 2010, **10**, 202–210.
23 J. Yang, Y. Liu and C. B. Rauch, *Lab Chip*, 2002, **2**, 179–187.
24 J. Chen, M. Wabuyele and H. Chen, *Anal. Chem.*, 2005, **77**, 658–666.
25 J.-Y. Cheng, C.-J. Hsieh and Y.-C. Chuang, *Analyst*, 2005, **130**, 931–940.
26 D. L. House, C. H. Chon and C. Buddy Creech, *J. Biotechnol.*, 2010, **146**, 93–99.
27 K. Sun, A. Yamaguchi and Y. Ishida, *Sens. Actuators, B*, 2002, **84**, 283–289.
28 J.-Y. Cheng, M.-H. Yen and C.-T. Kuo, *Biomicrofluidics*, 2008, **2**, 024105.
29 J.-L. Lin, M.-H. Wu and C.-Y. Kuo, *Biomed. Microdevices*, 2010, **12**, 389–398.
30 S. Kumar Jha, R. Chand and D. Han, *Lab Chip*, 2012, **12**, 4455–4464.
31 G. Pirri, F. Damin and M. Chiari, *Anal. Chem.*, 2004, **76**, 1352.
32 B. Ding, B. Kull and Z. Liu, *Regul. Pept.*, 2005, **127**, 45–53.
33 M. Heilig, O. Zachrisson and A. Thorsell, *J. Psychiat. Res.*, 2004, **38**(2), 113–20.

34 A. Ukkola and Y. A. Kesäniemi, *Eur. J. Clin. Nutr.*, 2007, **61**, 1102–1105.
35 M. Cretich, V. Sedini and F. Damin, *Sens. Actuators, B*, 2008, **132**, 258–264.
36 M. Cretich, V. Sedini and F. Damin, *Anal. Biochem.*, 2010, **397**, 84–88.
37 J. Miwa, Y. Suyiki and N. Kasagi, *JMEMS*, 2008, **17**(3), 611–622.
38 E. M. Robinson, R. Lam and E. D. Pierstorff, *J. Phys. Chem. B*, 2008, **112**(37), 11451–11455.